A HYPOTHESIS ON CONCEALED MAGMATISM IN SOUTHERN TIBET

Hirofumi MURAOKA[1], Osamu ISHIZUKA[2], Jian CHEN[3], SUOJIA[3] and Shin'ichi MIYAZAKI[4]
[1]AIST, Institute for Geo-Resources and Environment, 1-1-3 Higashi, Tsukuba, Ibaraki 305-8567, Japan
[2]AIST, Institute of Geology and Geoinformation, 1-1-3 Higashi, Tsukuba, Ibaraki 305-8567, Japan
[3]Tibet Geothermal Geological Team, Tibet Bureau of Geology and Mineral Exploration and Development, Lhasa 850032, Tibet, China
[4]Japan Metals & Chemicals Co., Ltd., 1-17-25 Shinkawa,Chuo-ku, Tokyo 104-8257, Japan
E-mail: hiro-muraoka@aist.go.jp

ABSTRACT

High-temperature geothermal resources are known along extensional grabens in southern Tibet where a well reached 329.8 ºC at a depth of 1850 m and seismological studies detected a partially molten layer at a depth form 15 to 18 km. Nevertheless, neither Plio-Pleistocene volcanoes nor Plio-Pleistocene volcanic rocks are observed at the surface, suggesting that magmatism is concealed without any eruptions in southern Tibet. A new $^{40}Ar/^{39}Ar$ age, 10 Ma, obtained on a possible volcanic edifice in Yanyi also supports this idea. A special tectonic situation in Tibet is that the deeper zone is constrained by contraction tectonics due to continental collision and the shallower zone is constrained by extension tectonics due to gravity collapse. A hypothesis is proposed on the density and stress profiles on the special tectonic regime in Tibet. According to the analysis, the buoyancy-driven magma rise is constrained by the low density host rocks at the shallow depth due to extension tectonics and the pumping type magma rise is difficult to occur by the high tectonic stress at the greater depth due to contraction tectonics. Therefore, the buoyancy-driven magma bodies could be only expected along the grabens at a several kilometer depth in southern Tibet.

Keywords: southern Tibet, concealed magmatism, neutral buoyancy depth, graben, tectonics, volcano, geothermal resources.

1. INTRODUCTION

High-temperature geothermal fields are known in southern Tibet, China, such as Nagqu, Guru, Ningchon, Yangbajain and Yanyi. They are distributed with an average spacing of 62.5 km along an extensional graben, totally 250 km long from Nagqu to Yanyi in the NE-SW direction. Since the Tibet Railway is now constructing along this graben, electricity demands will rapidly increase in the area, where one of the most potential candidates for energy sources would be geothermal power developments.

Seismological surveys conducted by a team of USA, Germany, Canada and the Chinese Academy of Geosciences in the INDEPTH project proposed a partially molten layer beneath the Nagqu-Yanyi graben at a depth form 15 to 18 km (Brown et al., 1996; Nelson et al., 1996; Makovsky et al., 1996; Kind et al., 2002; Spratt et al., 2005). A well ZK4002 drilled to a depth of 2006.8 m in Yangbajain recorded the highest temperature of 329.8 ^{0}C at a depth of 1850 m (Tibetan Geothermal Development Company, 1995). All the data indicate that the Nagqu-Yanyi graben is believed to have active magmatism at a depth.

Nevertheless, any young volcanoes are not known at the surface in the Nagqu-Yanyi graben as well as in southern Tibet, except for the Tengchong geothermal field, Yunnan, far south and almost outside of the Tibet plateau. This is one of the enigmas on magmatism in the Tibet plateau.

This paper shows a new $^{40}Ar/^{39}Ar$ age data of a volcanic rock sample taken from a possible volcanic edifice in the Yanyi geothermal field and proposes a hypothesis on the enigma of the concealed magmatism in southern Tibet.

2. PREVIOUS WORKS ON TECTONICS IN TIBET

Tibet is Earth's largest and highest plateau (Tapponnier et al., 2001), the extent of which is 3500 km in the EW direction and 1500 km in the NS direction, that is comparable with western Europe (Fig. 1). The altitude of the Tibet plateau is mostly close to 5000 m above sea level (Fig. 1). An analysis on the continent-continent collision tectonics in the Tibet plateau was initiated by a classical work of Molnar and Tapponnier (1975). This was followed by Coulon et al., (1986), Turner et al. (1993), Molnar et al. (1993), Fielding (1996) and Tapponnier et al. (2001). Molnar et al. (1993) show that a relative convergent velocity between the Eurasia and India continents had been 10 cm/year but has reduced to be 5 cm/year after 50 or 40 Ma. The initiation of the collision is then estimated to be 55 Ma. The collision tectonics has caused their crustal thickening by 80 km in Tibet.

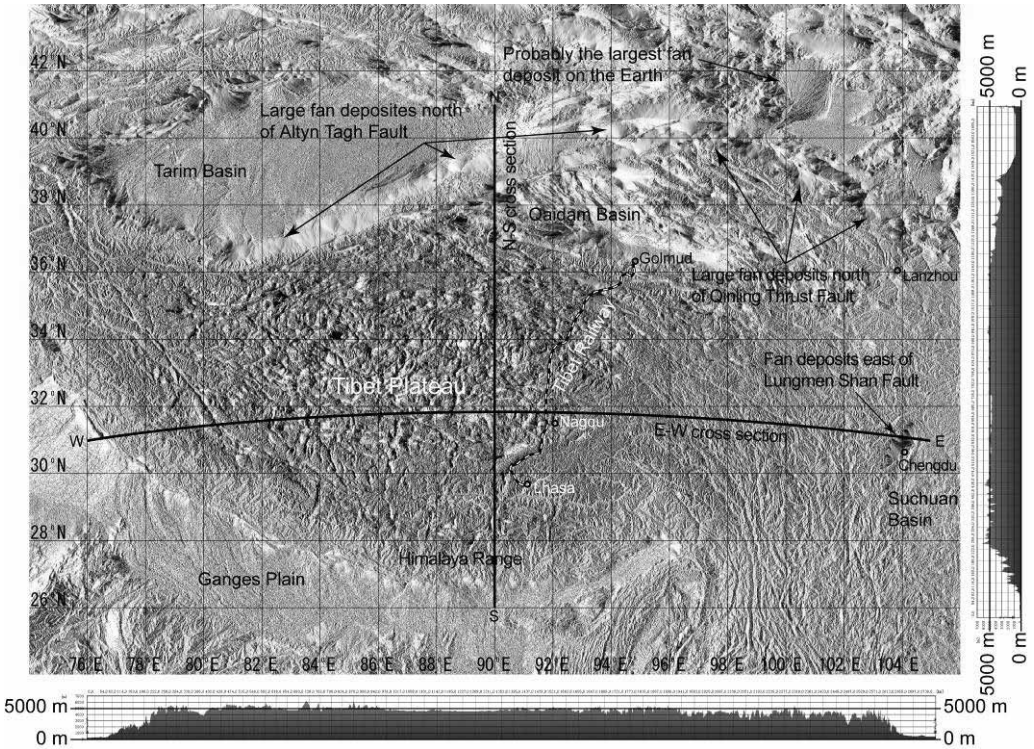

Fig. 1 Topography of the Tibet plateau. The SRTM 3 second data was used from USGS. Localities for cross sections are shown by the N-S and E-W lines on a plan view.

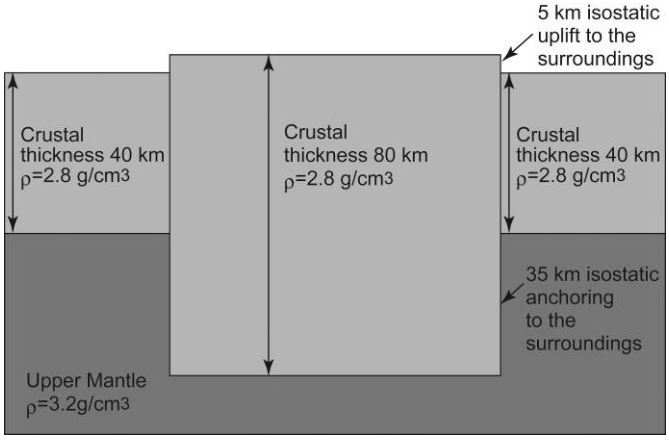

Fig. 2 A simple isostacy model of the Tibet plateau.

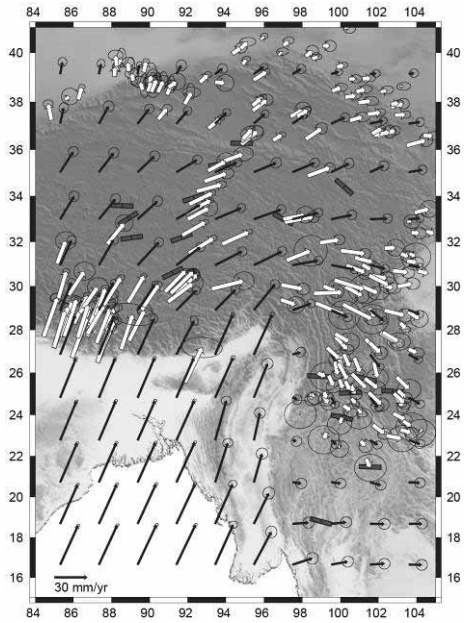

Fig. 3 Measured GPS motions (white arrow) and extrapolations in Tibet from Flesh et al. (2005).

When we assume the density of mantle to be 3.2 g/cm^3, the density of crust to be 2.8 g/cm^3 (Molnar et al., 1993), the thickness of crust in Tibet to be 80 km (Kind et al., 2002) and the thickness of normal crust in the surrounding regions to be 40 km, we obtain a simple isostacy (gravity equilibrium) model as shown in Fig. 2, where the relative uplift of the Tibet plateau to the surrounding regions is exactly 5000 m. There still remains a subject how a double crustal thickness was attained in Tibet. The current GPS data shows that the lateral motion strain is almost absorbed in the Tibet plateau from the south to north, from the southwest to northeast or from the west to east as shown in Fig. 3 (Flesh et al., 2005). This means that the crustal thickening driven by the lateral shortening is still continued at present and explains the crustal thickening process.

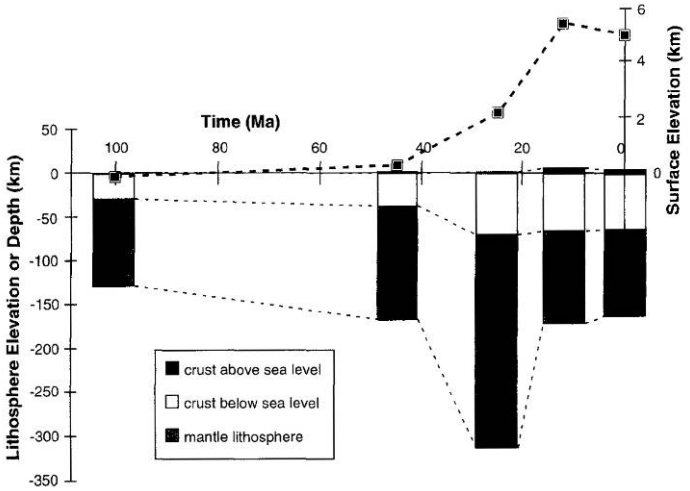

Fig. 4 Tibet isostatic uplift scenario from Fielding (1996).

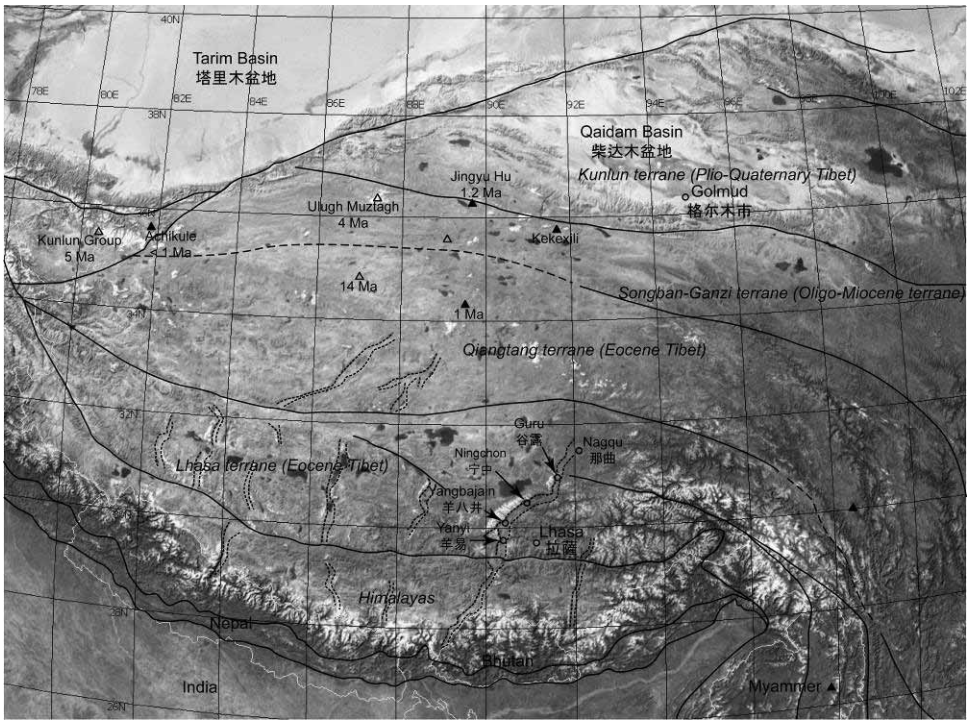

Fig. 5 Terrane subdivision of the Tibet plateau after Tapponnier et al. (2001). The base map is a satellite composite image taken from the World Wind, NASA. Some volcanoes are described on the image.

The crustal thickening is considered to have mainly occurred from 55 Ma to 10 Ma and to have been almost completed by 10 Ma (Molnar et al., 1993), although the GPS data suggest presently ongoing thickening (Fig. 3). On the other hand, the uplifting of the Tibet plateau is considered to have rapidly occurred from 13 Ma to 8 Ma (Molnar et al., 1993). An example of the temporal estimate on the crustal thickening and uplifting in the Tibet plateau is shown in Fig. 4 (Fielding, 1996).

Figure 5 shows that the Tibet plateau is divided into a several terranes by large-scale faults or suture zones (Tapponnier et al., 2001). As mentioned, the Tibet plateau is basically constrained by the NE-SW contraction tectonics, but interesting is the fact that there are also a several extensional grabens trending in the NE-SW direction (Fig. 5; Armijo et al., 1986; 1989). These grabens are mainly developed in the Lhasa terrane, partly extended to the Qiangtang terrane at the north and the Himalayas terrane at the south. One of these grabens is the Nagqu-Yanyi graben concerned. The timing for the initiation of these extensional grabens was estimated to be 8 Ma (Molnar et al., 1993). Molnar et al. (1993) explain that this event reflected downward removal of deeper lithosphere replaced by hotter asthenosphere from

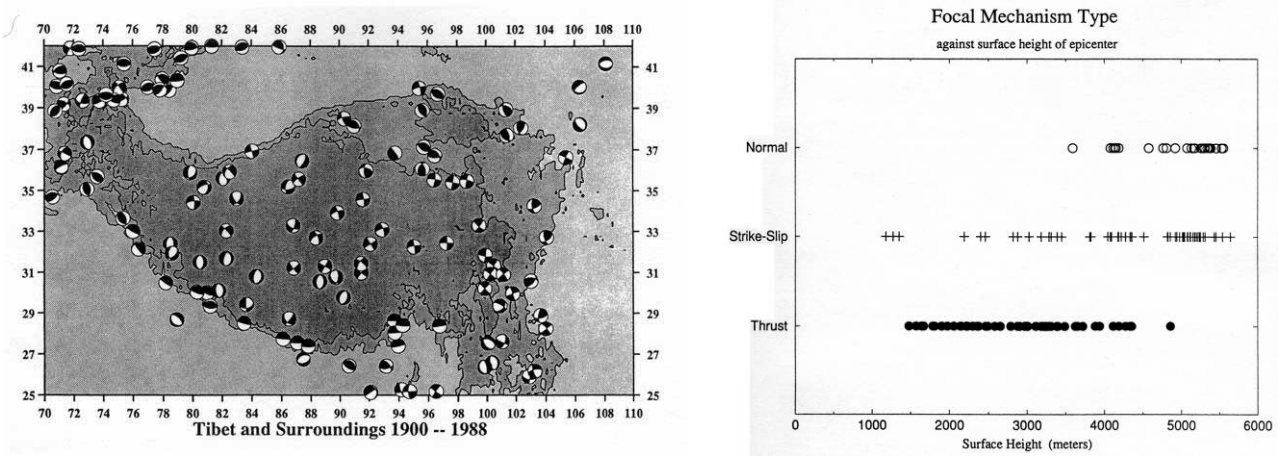

a) b)

Fig. 6 Explanations for coexistence of contraction and extension tectonics in Tibet from Molnar et al. (1993). a) Distribution of focal mechanisms in Tibet. b) Focal mechanisms versus elevations of epicenters in Tibet.

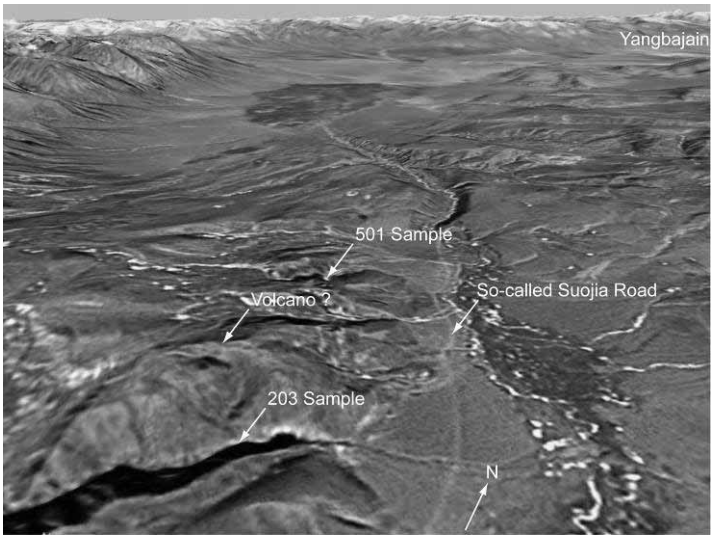

Fig. 7 An oblique satellite view of the Yanyi geothermal field 203 and a possible volcanic edifice.

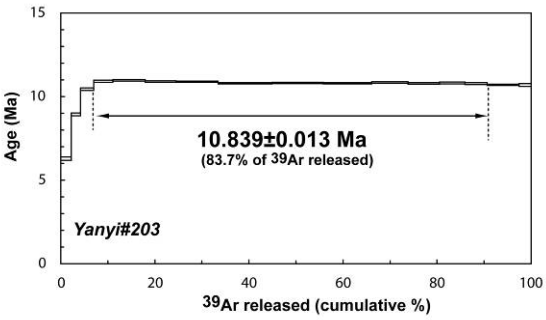

Fig. 8 Result of the $^{40}Ar/^{39}Ar$ age dating on the Sample. See Fig. 7 for the locality.

13 Ma to 8 Ma.

A paradoxical assembly of the NE-SW contraction tectonics and the extensional graben tectonics is clearly explained by Molnar et al. (1993). Figure 6a shows focal mechanisms of earthquakes in Tibet (Molnar et al., 1993). Normal fault type earthquakes are concentrated in the Lhasa terrane. When we compare the altitude of each earthquake epicenter (not hypocenter) and its focal mechanism, the type of focal mechanism depends on the altitude of the epicenter as shown in Fig. 6b. Most of the thrust fault type earthquakes are observed at the altitude below 4500 m. Most of the normal fault type earthquakes are observed at the altitude above 4000 m. Based on the data, Molnar et al. (1993) suggest that the highly uplifted area cannot support the overburden stresses to its margins and crustal thinning should have lowered the mean elevation. This effect is a sort of gravity tectonics or gravity collapses that explain a mechanism to maintain the mirror-like flat surface on the Tibet plateau.

Chronological studies on volcanic rocks show that the relatively young volcanoes are only known in northern Tibet (Fig. 5; Coulon et al., 1986; Turner et al., 1993, 1996; Tapponnier et al., 2001; Hou et al., 2004). They are mostly clusters of monogenetic volcanoes that appeared between 13 and 0 Ma and are not necessarily prospective as geothermal heat sources. In the Lhasa terrane, southern Tibet, paroxysmal Cenozoic volcanism occurred between 60 and 50 Ma (Coulon et al., 1986). This magmatism probably reflects the incipience of the continent-continent collision tectonics at 55 Ma. The youngest episode of volcanism in the Lhasa terrane occurred between 18 and 10 Ma (Coulon et al., 1986; Hou et al., 2004). When we consider the high-temperature geothermal activity in southern Tibet, the lack

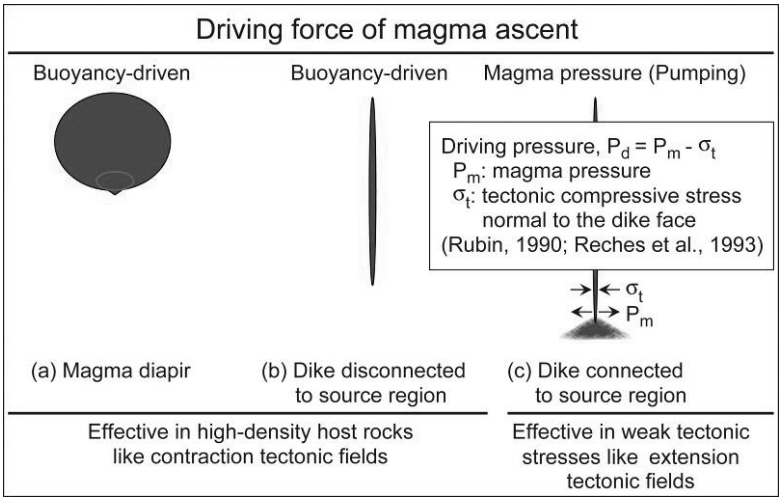

Fig. 9 Background of magma ascent.

of young volcanoes at the surface is one of the enigmas on magmatism in the area.

3. A NEW AGE OF A POSSIBLE VOLCANIC EDIFICE IN YANYI

Figure 7 shows a possible volcanic edifice in the Yanyi geothermal field. Two samples of andesite lavas were taken from the localities shown on the figure, July 2005. The age measurements are still ongoing, but a preliminary result on one sample taken from the locality near a well ZK203 (Liao and Zhao, 1999) is here described. The age measurement was done by the laser heating $^{40}Ar/^{39}Ar$ dating technique and the details of the method are described in Uto et al. (1997). The measurement was done on the volcanic glass.

The sampling site is situated at the southern part of the Yanyi geothermal field, and is surrounded by many high-potential geothermal wells (Liao and Zhao, 1999). In addition, the locality is situated at the southern foot of a possible volcanic edifice (Fig. 7). We expected a relatively young age, compared to those of the previous studies. However, the obtained result is 10.839±0.013 Ma (Fig. 8). The plateau shape on Fig. 8 shows the reliability of the age. This age is in the range reported by Coulon et al. (1986). The mean annual precipitation in Tibet is between 200 and 500 mm. Old volcanic edifices are sometimes preserved in such an arid area. The result again supports the concealed magmatism in southern Tibet.

4. DISCUSSION

Concealed Magmatism in Southern Tibet

As described above, seismological surveys proposed a partially molten layer beneath the Nagqu-Yanyi graben at a depth form 15 to 18 km (Brown et al., 1996; Nelson et al., 1996; Makovsky et al., 1996; Kind et al., 2002; Spratt et al., 2005). A well ZK4002 drilled to a depth of 2006.8 m in Yangbajain recorded the highest temperature of 329.8 ^{0}C at a depth of 1850 m (Tibetan Geothermal Development Company, 1995). Such a high-temperature hydrothermal convection system inevitably requires relatively young magma chambers at a depth from a few to a several kilometers. Nevertheless, there are not any young volcanoes at the surface in southern Tibet. The present preliminary age dating also supports this viewpoint. Therefore, only a possible solution seems concealed magmatism where most of magma chambers are emplaced at a greater depth with neither volcanoes nor eruptions.

Background of Magma Ascent

Magma may rise (a) in a diapir, (b) in an elastic dike disconnected from a magma source region or (c) in an elastic dike connected to the magma source region. There is a critical difference between magma in a diapir or a disconnected dike, which can only rise if it is buoyant, and magma in a connected dike, which can rise even when it is not buoyant if the source region has a great enough over-pressure (Fig. 9; Wilson et al., 1993).

The (a)- and (b)-types are exclusively constrained by the buoyancy of magma in the crust. The buoyancy is evaluated by the density contrast between the magma and surrounding rocks. An effect of density variation with magma composition was discussed by Muraoka (1997). An effect of density of surrounding rocks in the shallow crust was discussed by Muraoka and Yano (1998) and Muraoka (1998). At a depth less than several kilometers, the density of rocks greatly increases with depth, because the porosity of rocks dramatically decreases with depth. The porosity change is, strictly speaking, a function of anisotropic stress rather than of isotropic pressure.

Even at the same depth, anisotropic stress is quite different between contraction and extension tectonic fields. Muraoka

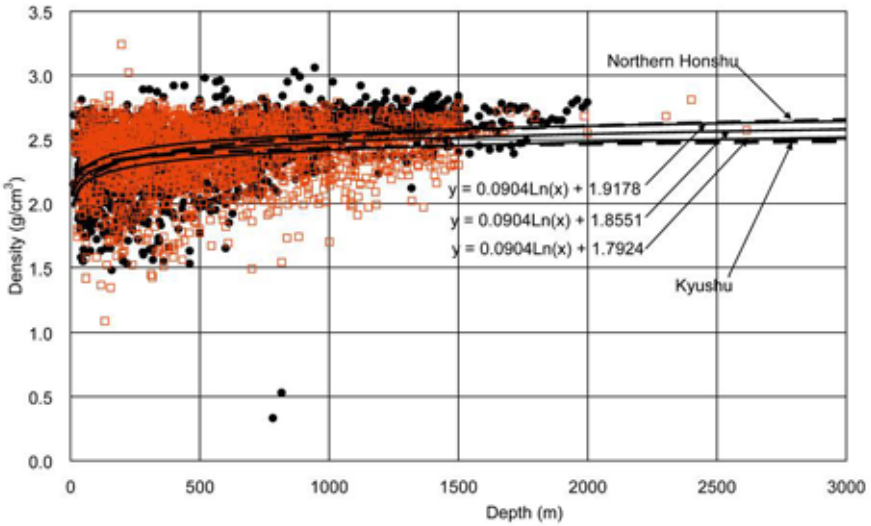

Fig. 10 Density comparison of core samples in northern Honshu (closed circle) and Kyushu (open square) modified from Muraoka and Yano (1998) and Muraoka (1998).

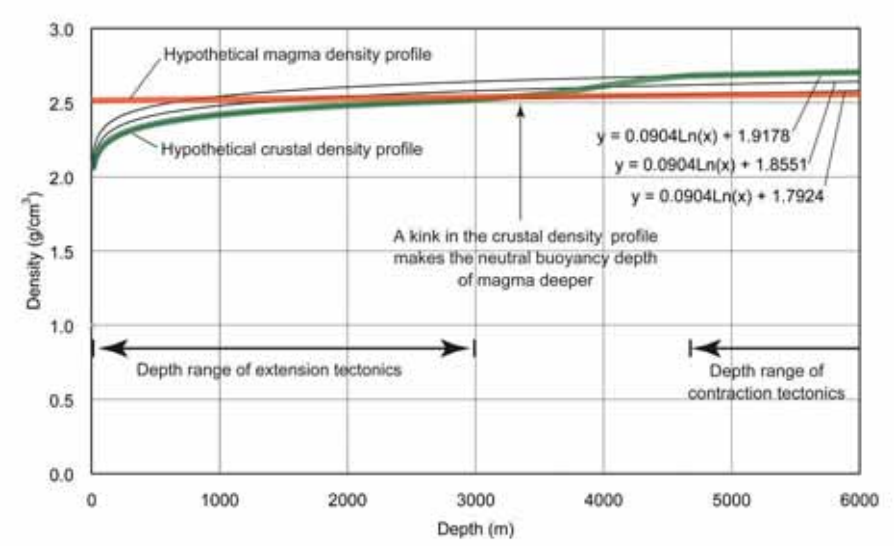

Fig. 11 A hypothetical density profile in the Tibet plateau.

and Yano (1998) and Muraoka (1998) compared the density of rocks between northern Honshu as a typical contraction tectonic field and Kyushu as a typical extension tectonic field as shown in Fig. 10. The density of rocks is larger in northern Honshu and smaller in Kyushu as expressed by each regression curve with depth. They are, however, difficult to compare the exact depth effect. Therefore, a regression curve on the total clusters from both fields was once drawn as a normalized curve, and then, the curve was proportionally changed only on the depth axis (Fig. 10). As a result, a normalized density profile of northern Honshu is approximated as $y = 0.0904\mathrm{Ln}(x) + 1.9178$ and that of Kyushu as $y = 0.0904\mathrm{Ln}(x) + 1.7924$. These equations indicate that the same density value is obtained at an exactly four times greater depth in Kyushu than in northern Honshu. This effect makes a neutral buoyancy depth of the (a)- and (b)-type's magma bodies four times deeper in Kyushu than in northern Honshu. This explains the reason why young plutonic bodies are shallower in contraction tectonic fields (Muraoka and Yano, 1998; Muraoka, 1998).

The (c)-type magma is analyzed in terms of driving pressure, $P_d=P_m-\sigma_t$, where P_m is the magma pressure at a depth of the magma source region and σ_t is the tectonic compressive stress normal to the dike face (Rubin, 1990; Reches et al., 1993). Because the vertical (overburden) stress is a standard value to divide compressive or extensive stress and is almost equal to σ_1 in the extension tectonic fields, horizontal compressive tectonic stress σ_t is usually negative in the extension tectonic fields. Therefore, the driving pressure P_d is usually positive in the extension tectonic fields, allowing the magma to propagate to a shallow depth (Rubin, 1990; Reches et al., 1993). This rising process is similar to pumping. This explains a fundamental genesis of the rift-zone magmatism where dike swarms are the most dominant magmatic expression as seen in Iceland.

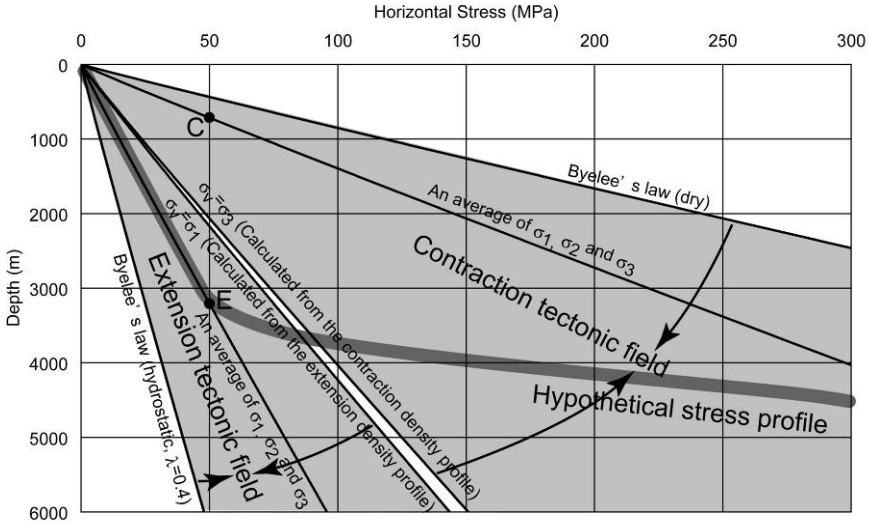

Fig. 12 A hypothetical stress profile in the Tibet plateau.

A Hypothesis on Concealed Magmatism in Tibet

Representing the density data of the contraction and extension tectonic fields by northern Honshu and Kyushu, a hypothetical density profile of Tibet is drawn in Fig. 11. A special tectonic situation in Tibet is that the deeper zone is constrained by contraction tectonics due to continental collision and the shallower zone is constrained by extension tectonics due to gravity collapse. The latter might be only effective above sea level. As shown in Fig. 11, the (a)- and (b)-type's magma bodies are constrained by a kink of the density profile that makes the neutral buoyancy depth of magma deeper.

A hypothetical stress profile of Tibet is drawn in Fig. 12. The σ_v is calculated from the density profiles of northern Honshu and Kyushu using $\sigma_v=\rho gz$, so that σ_v itself is larger in contraction tectonic fields and smaller in extension tectonic fields, more enhancing their stress difference. Although the diagram is conceptually drawn by the Byelee's law (Brace and Kohlstedt, 1980), a mean stress point E averaging anisotropic stresses in extension tectonic fields are roughly four times deeper than a mean stress point C in contraction tectonic fields. It is compatible with a density relation in Fig. 10. The hypothetical stress profile of Tibet is rather speculative, but it is obvious that a dramatic stress change with depth is necessary to attain contraction tectonics at the deeper zone and extension tectonics at the shallower zone. Ascending of the (c)-type magma bodies needs extension tectonics at a depth of the magma source region and it seems impossible in the stress regime in Tibet.

The (a)- and (b)-type's magma bodies are difficult to rise to a shallow depth and the (c)-type magma bodies are difficult to occur. These duplicated constraints could be a cause of the concealed magmatism in Tibet.

5. SUMMARY

High-temperature geothermal resources are known along extensional grabens in southern Tibet where a well reached 329.8 ^{0}C at a depth of 1850 m and seismological studies detected a partially molten layer at a depth form 15 to 18 km. Nevertheless, neither Plio-Pleistocene volcanoes nor Plio-Pleistocene volcanic rocks are observed at the surface, suggesting that magmatism is concealed without any eruptions in southern Tibet. A new $^{40}Ar/^{39}Ar$ age, 10 Ma, obtained on a possible volcanic edifice in Yanyi also supports this idea. A special tectonic situation in Tibet is that the deeper zone is constrained by contraction tectonics due to continental collision and the shallower zone is constrained by extension tectonics due to gravity collapse. A hypothesis is proposed on the density and stress profiles on the special tectonic regime in Tibet. According to the analysis, the buoyancy-driven magma rise is constrained by the low density host rocks at the shallow depth due to extension tectonics and the pumping type magma rise is difficult to occur by the high tectonic stress at the greater depth due to contraction tectonics. Therefore, the buoyancy-driven magma bodies could be only expected along the grabens at a several kilometer depth in southern Tibet.

REFERENCES

Arimjo, R., Tapponnier, P., Mercier, J.L. and Han, T. (1986) Quaternary extension in southern Tibet: Field observations and tectonic implications. *J. Geophys. Res.*, **91**, 13803-13872.

Arimjo, R., Tapponnier, P. and Han, T. (1989) Late Cenozoic right-lateral strike-slip faulting in southern Tibet. *J. Geophys. Res.*, **94**, 2787-2838.

Brace, W.F. and Kohlstedt, D.L. (1980) Limits on lithospheric stress imposed by laboratory experiments. *J. Geophys. Res.*, **85**, 6248-6252.

Brown, L.D., Zhao, W., Nelson, K.D., Hauck, M., Alsdorf, D., Ross, A., Cogan, M., Ckark, M., Liu, X. and Che, J. (1996) Bright spots, structure, and magmatism in southern Tibet from INDEPTH seismic reflection profiling. *Science*, **274**, 1688-1690.

Coulon, C., Maluski, H., Bollinger, C. and Wang, S. (1986) Mesozoic and Cenozoic volcanic rocks from central and southern Tibet: 39Ar-40Ar dating, petrological characteristics and geodynamical significance. *Earth and Planetary Science Letters*, **79**, 281-302.

Fielding, E.J. (1996) Tibet uplift and erosion. *Tectonophysics*, **260**, 55-84.

Flesch, L.M., Holt, W.E., Silver, P.G., Stephenson, M., Wang, C.Y. and Chan, W.W. (2005) Constraining the extent of crust–mantle coupling in central Asia using GPS, geologic, and shear wave splitting data. *Earth and Planetary Science Letters*, **238**, 248– 268.

Hou, Z.-Q., Gao, Y.-F., Qu, X.-M., Rui, Z.-Y. and Mo, X.-X. (2004) Origin of adakitic intrusives generated during mid-Miocene east-west extension in southern Tibet. *Earth and Planetary Science Letters*, **220**, 139-155.

Kind, R., Yuan, X., Saul, J., Nelson, D., Sobolev, S.V., Mechie, J., Zhao, W., Kosarev, G., Ni, J., Achauer, U. and Jiang, M. (2002) Seismic images of crust and upper mantle beneath Tibet: Evidence for Eurasian plate subduction. *Science*, **298**, 1219-1221.

Liao, Z. and Zhao, P. (1999) *Yunnan-Tibet Geothermal Belt*. Science Publishing House, Beijing, 153p (in Chinese with English abstract).

Makovsky, Y., Klemperer, S.L., Ratschbacher, L., Brown, L.D., Li, M., Zhao, W. and Meng, F. (1996) INDEPTH wide-angle reflection observation of P-wave-to-S-wave conversion from crustal bright spots in Tibet. *Science*, **274**, 1690-1691.

Molnar, P. and Tapponnier, P. (1975) Cenozoic tectonics of Asia: Effects of a continental collision. *Science*, **189**, 419-426.

Molnar, P., England, P. and Martinod, J. (1993) Mantle dynamics, uplift of the Tibetan Plateau, and the Indian monsoon. *Reviews of Geophysics*, **31**, 357-396.

Muraoka, H. (1997) Conceptual model for emplacement depth of magma chambers and genesis of geothermal systems. *Proc. 30th, Int'l. Geol. Congr.*, **9**, 143-155.

Muraoka, H. (1998) Magma-tectonic background of geothermal systems. *Proceedings of Asian Geothermal Energy '98*, 137-144.

Muraoka, H. and Yano, Y. (1998) Why neo-plutons are deeper in extension tectonic fields and shallower in contraction tectonic fields. *Proceedings 20th NZ Geothermal Workshop 1998*, 109-114.

Nelson, K.D., Zhao, W., Brown, L.D., Kuo, J., Che, J., Liu, X., Klemperer, S.L., Makovsky, Y., Meissner, R., Mechie, J., Kind, R., Wenzel, F., Ni, J., Nabelek, J., Leshou, C., Tan, H., Wei, W., Jones, A.G., Booker, J., Unsworth, M., Kidd, S.F., Hauck, M., Alsdorf, D., Ross, A., Cogan, M., Wu, C., Sandvol, E. and Edwards, M. (1996) Partially molten middle crust beneath southern Tibet: Synthesis of Project INDEPTH results. *Science*, **274**, 1684-1688.

Reche, Z., Fink, J.H. and Agnon, A. (1993) Control of dike emplacement by vertically-varying tectonic stresses. *EOS Trans.*, AGU, Spring Meet. Suppl., 291.

Rubin, A.M. (1990) A comparison of rift-zone tectonics in Iceland and Hawaii. Bull. Volcanol., 52, 302-319.

Spratt, J.E., Jones, A.G., Nelson, K.D., Unsworth, M.J. and INDEPTH MT Team (2005) Crustal structure of the India-Asia collision zone, southern Tibet, from INDEPTH MT investigations. *Physics of the Earth and Planetary Interiors*, **150**, 227-237.

Tapponnier, P., Xu, Z., Roger, F., Meyer, B., Arnaud, N., Wittinger, G. and Yang, J. (2001) Oblique stepwise rise and growth of the Tibet Plateau. *Science*, **294**, 1671-1677.

Tibetan Geothermal Development Company (1995) *Development of the geothermal resource in Tibet (leaflet)*. Tibetan Geothermal Development Company, 12p (in Chinese and English).

Turner, S., Hawkesworth, C., Liu, J., Rogers, N., Kelley, S. and van Calsteren, P. (1993) Timing of Tibetan uplift constrained by analysis of volcanic rocks. *Nature*, **364**, 50-54.

Turner, S., Arnaurd, N., Liu, J., Rogers, N., Hawkesworth, C., Harris, N., Kelley, S., van Calsteren, P. and Deng, W. (1996) Post-collision, shoshonitic volcanism on the Tibet Plateau: Implications for convective thinning of the lithosphere and the source of ocean island basalts. *J. Petrol.*, **37**, 45-71.

Uto, K., Ishizuka, O., Matsumoto, A., Kamioka, H. and Togashi, S. (1997) Laser-heating $^{40}Ar/^{39}Ar$ dating system of the Geological Survey of Japan: System outline and preliminary results. *Bull. Geol. Surv. Japan*, **48**, 23-46.

Wilson, L., Head, J.W. and Parfitt, E.A. (1993) Factors controlling the generation, ascent, storage and eruption of magma. *EOS Trans.*, AGU, Spring Meet. Suppl., 291.